ICAS 2016
30th Congress of the International Council of the Aeronautical Sciences
DCC, Daejeon, Korea ; September 25-30, 2016

AN EXPERIMENTAL STUDY OF MICRO-ELECTROMECHANICAL FLYING INSECT FLAPPING WINGS AERODYNAMIC PERFORMANCE

Pawel Czekalowski*, Krzysztof Sibilski, Andrzej Żyluk*****
***Institute of Aviation, Al. Krakowska 110/114, Warsaw, Poland**
****Air Force Institute of Technology, Ks. Boleslawa 6, Warsaw, Poland**
***** Air Force Academy, Dywizjonu 303, Deblin, Poland**

Keywords: *entomopter, flapping wings aerodynamics, wind and water tunnels measurements*

Abstract

Microelectromechanical flying insect (entomopter) is the one of the youngest group of aircraft. Aerodynamic phenomena during entomopter flight are still not well recognized. Present work concerns on experimental investigations of flapping wings robot (so called flapper), conducted in water tunnel. Flapper is dipterous mechanism, and each wing can perform various spherical motions (wings are rotated around point). The aim of work is to investigate, how the lift force, tangent force and necessary power for horizontal flight are changing due to various kinematics rules of wing motion. The experiment consist of measurements of hydrodynamic forces generated by entomopter wings. Test was performed for various pitch angle trajectories. In addition, pitching moment and lift force derivatives of the forward velocity were designated.

1 Introduction

Flapping wings aerodynamics recently has generated a great deal of interest and increasing research effort because of the potential application in Micro Air Vehicles (MAV). For this research, a first-of-its-kind mechanical flapping-wing apparatus that mimics insect-like flapping-wing motion has been designed and developed. This apparatus features a novel flapping mechanism which gives the wing three controllable degrees of freedom required to produce the three separate motions necessary for mimicking an insect-like flapping-wing trajectory: sweeping (side-to-side), plunging (up and down) and pitching (angle-of-attack variation). In this mechanism these three motions are *independently* controllable.

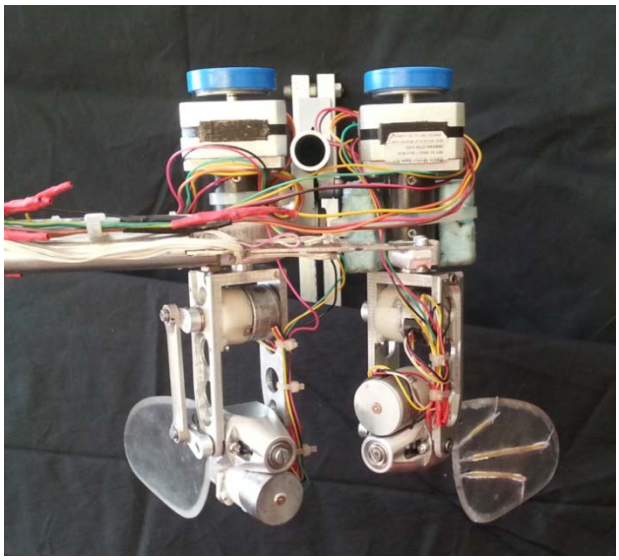

Fig. 1 Flapper - electromechanical flapping-wing apparatus that mimics insect-like flapping-wing motion

The present mechanism not only enables this but also a very wide range of other insect-like flapping kinematics to be achieved, as pictured in fig. 1. In contrast, our past mechanical flapper [6] have had fixed kinematics wings with only two degrees-of-freedom. This new apparatus, therefore, enables flapping-wing experiments which have never hitherto been performed.

2 Experiment set up

Experiments with the apparatus focused on observing and understanding the effects of varying flapping kinematics on the flows and

aerodynamic forces produced by the wings. For example, how does changing the angle-of-attack, or stroke amplitude (number of degrees swept by the wing in a flap), affect the lift and the flow structures? Such questions are of interest in Flapping Micro-Air Vehicles (FMAV) development because it is essential to know what type of flapping kinematics are appropriate to produce high lift. Experiments were conducted in the Low Reynolds Number Laboratory of the Wroclaw University of Technology (fig. 2).

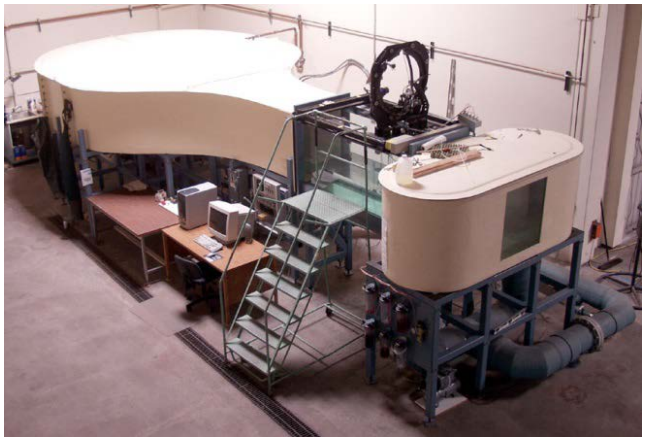

Fig. 2 The RHRC water tunnel model 2436

This laboratory is equipped with the Rolling Hills Research Corporation (RHRC) Model 2436 water tunnel. This is a closed circuit continuous flow, horizontal configuration device with a free surface. The horizontal free surface configuration allows model and instrumentation installation and access to be performed without draining the tunnel. The test section has a width of 24 inches, height of 36 inches, and length of 74 inches. The test section flow velocity is variable from 0 to 1.2 ft/s. This tunnel is equipped with honeycomb and screens along with a contraction ratio of 6:1 to provide high flow quality and low free-stream turbulence levels. The RHRC Model 2436 water tunnel has been used extensively for performing quantitative 3-D dynamic experiments using a submersible 5-component strain gage balance [1]. These dynamic experiments include forced oscillation motions, ramp and hold maneuvers, rotary balance tests, Schroeder sweeps, and Tobak-Schiff motions [1]. It was utilized dedicated visualization system to observe flow around the flapping-wing driven by the apparatus. Visualization system employs pressured multicolor seeding system and high-speed cameras to observe instantaneously all three flow velocity components over a grid of points within the measurement plane. Lift measurements were accomplished with a strain-gauge force balance fitted to the apparatus (fig. 3). These techniques enabled a parametric study in which various flapping kinematic parameters (angle-of-attack, stroke amplitude, flapping frequency etc.) were varied, and the resulting changes in the mean lift and flows produced were measured.

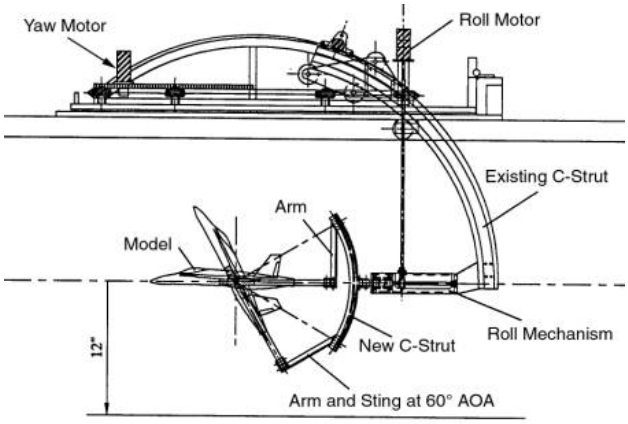

Fig. 3 The 3-axis model support system

To measure the forces on the model in the water tunnel a 5 component balance is available with a maximum diameter of 13 mm and a length of 167.5 mm, which uses high-sensitivity semi-conductor strain gages (fig. 4). High sensitivity is required because the model loads encountered in water tunnels are quite small.

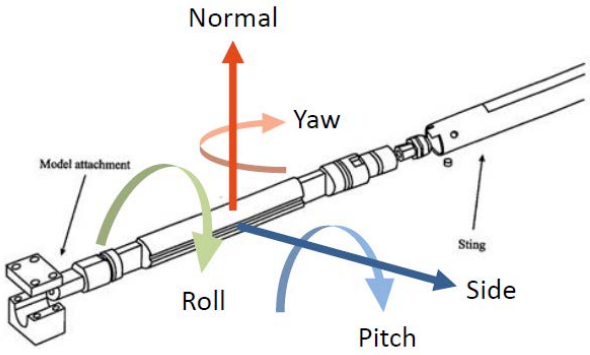

Fig. 4 Five components aerodynamic nalance

The flapper kinematics is shown in the fig. 5. The 3DOF system controlled three angular motions: pitch motion (γ), dihedral motion (θ)

and sweep motion (ϕ). The standard terminologies and nomenclatures used in fixed wing aerodynamics are adopted here. Three angles are taken as the motion parameters, (i.e. angles γ, θ, and ϕ), corresponding to feathering motion angle, elevation angle and position angle in some bioflight literature [2, 3, 5].

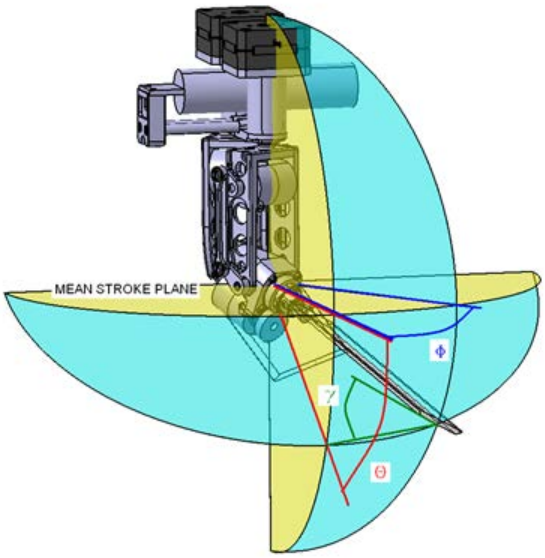

Fig. 5 Kinematics of flapper - mechanical flapping-wing apparatus

The time history of motion can be described by three equations and in case of this investigation are as follows:

$$\phi(t) = \Phi\sum_{i=1}^{N}\left[A_i\cos(2i\pi ft) + B_i\sin(2i\pi ft)\right]$$

$$\theta(t) = \Theta\sum_{i=1}^{N}\left[A_{\theta i}\cos(2i\pi ft) + B_{\theta i}\sin(2i\pi ft)\right] \quad (1)$$

$$\gamma(t) = \Gamma(k)\sum_{i=1}^{N}\left[A_i\cos(2i\pi ft) + B_i\sin(2i\pi ft)\right]$$

Entomopter produce lift and thrust forces by cyclic revolution of wings. Motion of wing is complicated, it is combination of revolutions around three axes. Azimuthal position of wing and angle of attack are changed simultaneously. Entomopter as insects operates in low Reynolds numbers regime (1000 – 10.000). Investigations on insects aerodynamic indicated phenomenon specific only for this regime [10, 13, 14, 15, 18, 23]. First attempts of aerodynamic modeling showed, that in reality insects produces higher forces than classical models predicted. Additionally behavior of aerodynamic loads in time course was unpredictable. Further investigation of flow field around insects-like wing showed, that key role in force production play detached or partially detached vortexes. The biggest impact on lift force in quasi steady motion have vortex generated by leading edge (Leading Edge Vortex) [11, 12, 15, 20, 21, 22, 23]. During reversal motion stages other aerodynamic phenomena became important. During this phase wing move with high acceleration. It effects with strong trailing edge vortex. High acceleration results also with high aerodynamic inertial forces (added mass effect). Superposition of those phenomenon makes impossible to predict correctly aerodynamic loads during complete cycle using simple quasi-steady methods. Nowadays we've got other, more precise tool: Computational Fluid Dynamic (CFD). CFD have capability to reproduce all of mentioned above effects. In literature types of analysis are present: two and three dimensional. Many papers describe results of 2-dimensional models [9, 13, 14, 18, 20, 21, 2226]. Conclusion of this works are, that despite of model simplification results are helpful for understanding of main aerodynamic mechanisms. In the other hand most of those analysis are performed for very low Reynolds numbers, below of regime of Re=1000). Second group of analysis are three dimensional cases. Most papers concerns on reproduction of insects aerodynamics [4, 6, 16, 20, 23, 24, 25].

To achieve comparable view of influence of previously defined geometrical parameters, (i.e. angles γ, θ, and ϕ), on resulting forces during water tunnel measurements, it is necessary to define similarity numbers:

- Reynolds number, which for 3D flapping motion is expressed as follows:

$$\mathrm{Re} = \frac{4f\Phi R^2}{\upsilon AR} \quad (2)$$

where: $AR = \frac{(2\cdot R)^2}{S}$,

- Stroke amplitude.
- Flapping frequency f:

$$f = \frac{\mathrm{Re}\,\upsilon AR}{4\Phi R^2} \quad (3)$$

In consequence mean Reynolds number was constant for one measurement series [6, 7].
For example, the time history of wing angular position (stroke angle) can be expressed as follows (see egs 1) [6, 7]:

$$\phi(t) = \frac{\Phi}{2}\sum_{i=1}^{N}\left[A_i \cos(2i\pi f(k)t) + B_i \sin(2i\pi f(k)t)\right] \tag{4}$$

If instead frequency f will be put equation 3, above expression will take a form [6, 7]:

$$\varphi(t) = \frac{\Phi}{2}\sum_{i=1}^{N}\left[A_i \cos(i\pi \frac{\mathrm{Re}\cdot\upsilon\lambda}{2\Phi R^2}t) + B_i \sin(i\pi \frac{\mathrm{Re}\cdot\upsilon\lambda}{2\Phi R^2}t)\right] \tag{5}$$

Basing on above, we can find, that both maximal and average angular velocitcies are constant during each series, because theirs value can be obtained from following expressions:

$$|\omega|_{\max} = \frac{\mathrm{Re}\,\upsilon\lambda\pi}{4R^2}, \quad |\bar{\omega}| = \frac{\mathrm{Re}\,\upsilon\lambda}{2R^2}. \tag{6}$$

In equations (6) linked parameters (frequency and amplitude) are absent [7, 8].

Robotics entomopter model (flapper) was mounted on support of water tunnel, and it was able to perform oscillatory motion around three axes, according to possibilities of wid tunnel support, see fig. 3, [1]. During experiments such oscillatory motion were performed relative to the pitch angle of flapper body. Flapper dynamic motion Frequency was the same as for the wing flapping frequency, (support and wing motions were correlated), and was equal 0.2Hz. Support performed sinusoidal motion with amplitude 10^o. Phase shift (*dt*) between wing and support oscillations was the parameter of the experiment. Maximal velocity of pitching motion was 0.2193 [1/s], maximal acceleration during this motion was 0.0138 [$1/s^2$]. Flapper has offset from support center of rotation equal 80mm. Two series of measurements were performed for two different positions of model. Each series consist of 10 measurements. During first model had offset along normal to mean stroke plane direction. As results we had obtained variation in tangent to stroke plane. For second series model has moved along tangent to stroke plane direction. In this way we can obtained effect of variation in normal to plane velocity plane [7].

3 Results of water tunnel tests

Results of water tunnel tests confirmed the presence of a leading-edge vortex (LEV) over the wing, which feeds into the tip vortex, as illustrated in Figure 6.

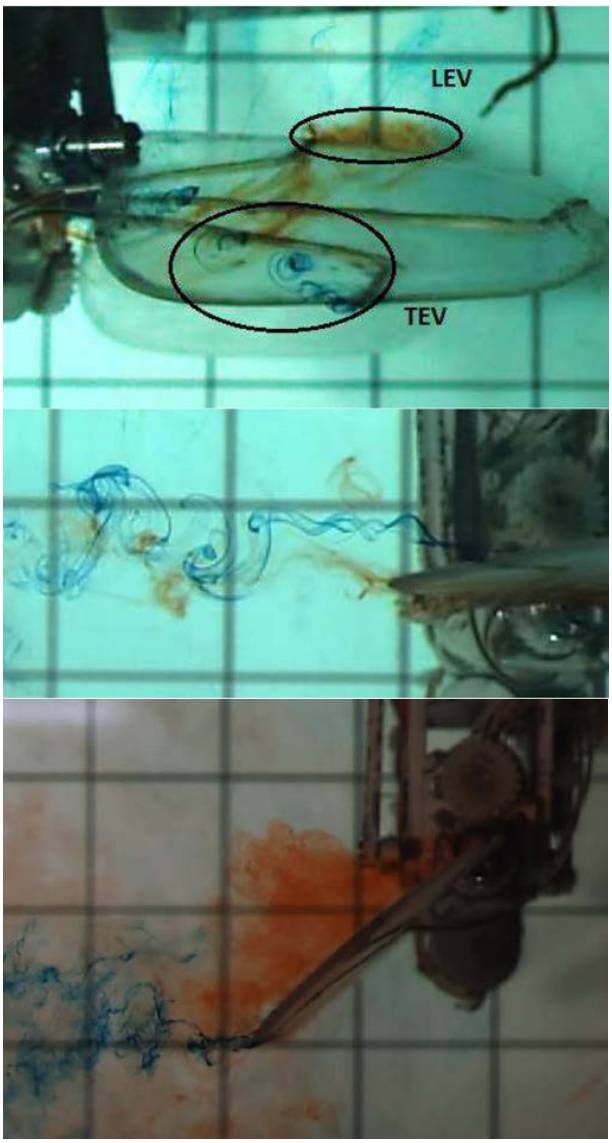

Fig. 6 Water tunnel flow visualization. There are shown vortex structures of trailing and leading edges of flapping wings

This is similar to the LEVs formed on delta wings, and its existence on flapping wings has been well established by previous researchers see for example works by Dickinson [10, 26], Ellington [11], or the latest works of Kudela and Kozlowski [18], and Ol [21, 22].
Results of measurements confirmed, that leading edge vortex (LEV) is the main method used by natural yers, especially at low Reynolds numbers, to maintain attached flow on the wing

at large angles of attack. It is dependent on the swirl strength, the rotational rates of the wing motion and the Reynolds number. The LEV attaches a bounded vortex core on the upper surface of the wing during the transitional stage (periods of the cycle when the wing is not pronating or supinating), which delays stall and thus allows for high angles of attack.

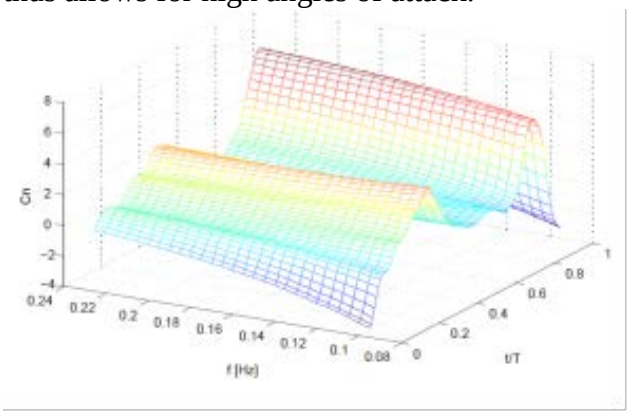

Fig..7 Measured normal force coefficient C_n as a function of flapping frequency and position of wing during the wingbeat cycle

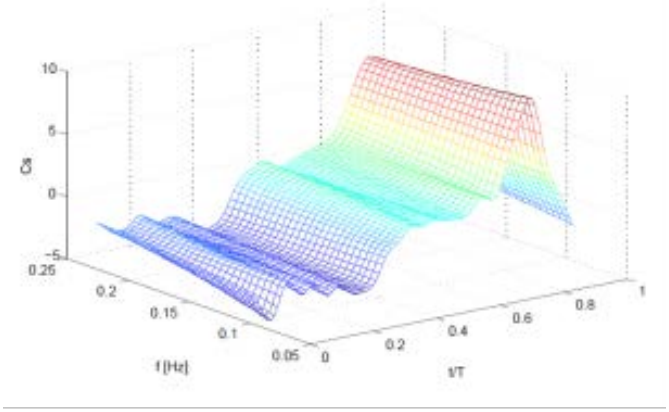

Fig. 8 Measured tangential force coefficient C_s as a function of flapping frequency and position of wing during the wingbeat cycle.

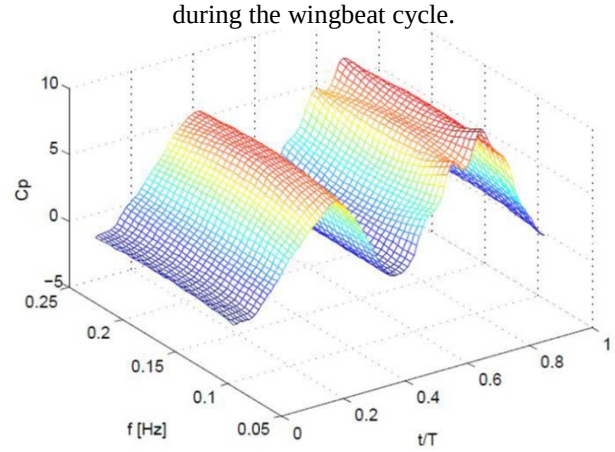

Fig. 9 Measured power coefficient Cp as a function of flapping frequency and position of wing during the wingbeat cycle.

Figures 7, 8, and 9 show results of measurements of normal, tangential force coefficients, and power coefficient, as function of flapping cycle and flapping frequency. The normal and tangential force coefficients are defined as follows:

$$C_n = \frac{N_{av}}{2\rho\pi^2(2\Phi)^2 f^2 \int_0^R \cdot r^2 \cdot c(y) \cdot dy}$$

$$C_s = \frac{T_{av}}{2\rho\pi^2(2\Phi)^2 f^2 \int_0^R \cdot r^2 \cdot c(y) \cdot dy} \qquad (7)$$

$$C_p = \frac{P}{4\rho \cdot (\pi f(2\Phi))^3 \cdot \int_0^R r^3 c(y) \cdot dy}$$

where: N_{av}, and T_{av} are average normal and tangent forces respectively, measured by the aerodynamic balance. P is the power necessary for propulsion of wing during one wingbeat cycle. Power was calculated taking into accout electric power consumption by the motor powered the flapping wing [6]. Φ is the stroke amplitude, and f is the flapping frequency.

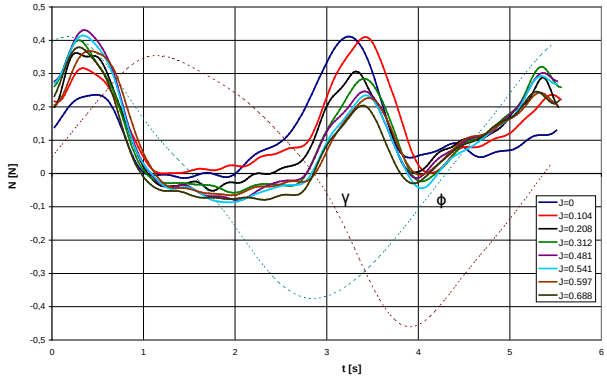

Fig. 10. Normal force component for various forward flight speeds

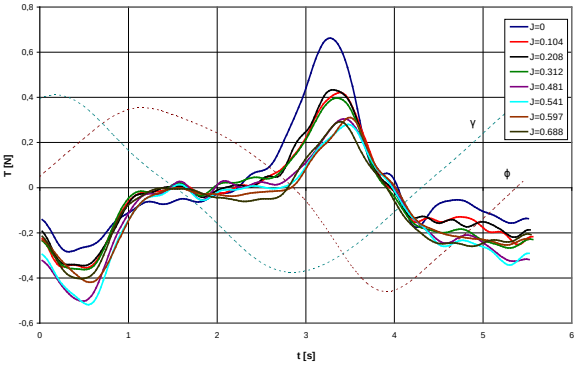

Fig. 11 Tangent force component for various forward flight speeds

Figures 7, 8, and 9 show, that efficiency of flapping wings are better for the higher frequencies' of flapping.
In figures 10. and 11 show summarized plots of normal and tangent force components for different forward flight speeds. Average horizontal force component (parallel to velocity vector) is near zero, so it can be assumed, that flight conditions are fixed. Increasing forward flight velocity caused in enlargement of values of normal force during upstroke and reduction during down stroke. Significant differences are during reversal. The higher was flight speed the lower values were achieved. For test with 0.54 advance ratio it seemed that had stopped. In every phase normal force is lower than in case test with lower speed (J=0.48).
The analysis of tangent component force shows that the biggest differences are for hover flight. This plat have is the most asymmetry, thus resultant force have the highest value. Differences between plots are quite similar. Also in case of the highest velocities differences are less significant than in case of rest.
Figures 12 show characteristics of average lift force coefficient (C_n) and tangential force coefficient (C_s) from measurement and CFD calculations as function of Reynolds number.

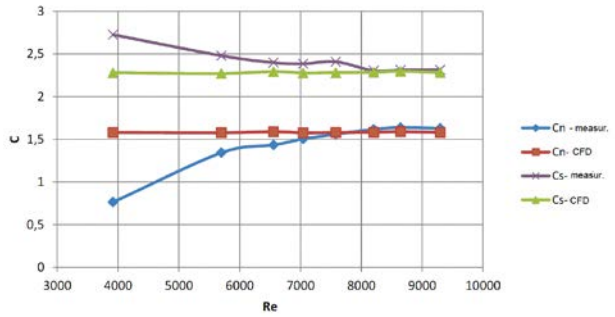

Fig. 12 Average normal and tangential force coefficient as function of Reynolds number, (measurements vs CFD calculations)

It can be stated, that when the Reynolds number is less than 7.000 the normal force coefficient is decreasing, and tangent force coefficient is increasing. CFD calculations (using unsteady VLM method show, that Teynolds number has not influence on average forces generated by the flapping wings.
We have conducted on water tunnel experiment an insect like wing performing 3-D-of-freedom motions. Experiments give very important tips, which will be useful during designing and developing process of electromechanical entomopter prototype. Tests proved, that linkage between geometrical and kinematics parameters is very strong and both parameters impact on resultant forces. Furthermore results have explained, why in insects world short wings are so popular. Unfortunately the range of variability of investigated parameters was quite narrow. In near future experiment will be continued. Wings with smaller aspect ratio will tested and torque (which was also measured) also will be analyzed.

4 Conclusions

From aerodynamic point of view top speed haven't been exceeded during experiment. Analysis of resultant forces have not demonstrated any changes, could evidence, that entomopter cannot fly faster. It is difficult to predict behavior of the object during flight with higher velocities. Probably it could increase speed up to moment, when pitch angle will be 90 degrees (mean stroke plane perpendicular to velocity vector). After that point further acceleration will be possible only by increasing flapping frequency. Changing pitch angle (PA) appears to be enough efficient way for steering for accelerating. During test it turned out, that lift force is changing with forward flight speed. Definitely presented data should be completed with measurements of necessary power to moving wing of robot. Presented results can be used for quasi – steady aerodynamic model used for dynamic motion analysis.

References

[1] Animus, RHRC Research water tunnel specification, El Segundo California, User's Manual, 2009.
[2] Ansari, A. S., Żbikowski, R., Knowles, K., "Aerodynamic modelling of insect-like flapping flight for micro air vehicle," *Progress in Aerospace Sciences*, vol. 42. pp. 129-172, 2006.
[3] Ansari, S. A., Knowles, K., Żbikowski, R., "Insectlike flapping wings in the hover part 1, and 2: effect of wing kinematics," *Journal of Aircraft*, Vol. 45, No. 6, 2008.
[4] Birch, M. J., Dickinson, M. H., Spanwise flow and the attachment of the leading-edge vortex on insect wings," *Nature*, Vol. 412 16, 2001.

[5] Conn, A., T., Chung Seng Ling, Burgess, S., C., "Biomimetic Analysis of Insect Wing Kinematics for Flapping MAVs," *The International Journal of Micro Air Vehicles*, Vol. 3m No. 1, pp. 1 – 11, 2011.
[6] Czekalowski, P., "Influence of Wing Motion Kinematics on Aerodynamic Loads of an Entomopter," Ph.D. Dissertation, Mechanics and Power Engineering Depy., Wroclaw University of Technology, Wroclaw, Poland, http://www.dbc.wroc.pl/dlibra/docmetadata?id=30239&from=publication, (in Polish), 2014.
[7] Czekalowski, P., Gronczewski, A., Sibilski, K., "Water tunnel experimental investigation on the aerodynamic performance of flapping wings for nano air vehicles," *AIAA online proceedings*, http://dx.doi.org/10.2514/6.2011-3789.
[8] Czekalowski, P., Sibilski, K., Zyluk, A., "Influence of Cruise Flight Speed of Entomompter on Aerodynamics Loads." *AIAA online proceeding*, http://dx.doi.org/10.2514/6.2013-770.
[9] Di, W., Khoon, Y., Seng, L. Tee Tai, "CFD Modeling of Insect Flight at Low Reynolds Number," *International Journal of Mechanical, Aerospace, Industrial and Mechatronics Engineering*, Vol:8, No:6, 2014.
[10] Dickinson, M. H., Gotz, K., "Unsteady aerodynamic performance of model wings at low Reynolds numbers," *Journal of Experimental Biology*, No, 174, pp. 45–64, 1993.
[11] Ellington, C., "The aerodynamics of hovering insect flight. I. The quasi-steady analysis," *Philosophical Transactions of the Royal Society*, vol. 305, str. 1-15, 1984
[12] Hao Wang, Lijiang Zeng, Hao Liu, Chunyong Yin, "Measuring wing kinematics, flight trajectory and body attitude during forward flight and turning maneuvers in dragonflies," *The Journal of Experimental Biology*, No. 206, doi:10.1242/jeb.00183, 2002, pp. 745-757.
[13] Hikaru Aono, Wey Shyy, Hao Liu, "Vortex Dynamics in Near Wake of a Hovering Hawkmoth," *AIAA online proceedings*, http://dx.doi.org/10.2514/6.2008-583.
[14] Hikaru Aono, Wey Shyy, Hao Liu, *Aerodynamics of low Reynolds number flyers*, Cambridge University Press, 2007.
[15] Hiroto Nagai, Koji Isogai, "Effects of Flapping Wing Kinematics on Hovering and Forward Flight Aerodynamics," *AIAA Journal*, Vol. 49, No. 8, DOI: 10.2514/1.J050968, August 2011.
[16] Jin-Ho Kim, Chongam Kim, "Unsteady Flowfields Characteristics around Two- and Three-dimensional Flapping Flight," *AIAA online proceedings*, http://dx.doi.org/10.2514/6.2008-6400.
[17] Keennon, M., Klingebiel, K., Won, H., Andriukov, A., "Development of the Nano Hummingbird: A Tailless Flapping Wing Micro Air Vehicle," *AIAA online proceedings*, http://dx.doi.org/10.2514/6.2012-588, 2012.
[18] Kudela, H., Kozlowski, T., "Hydrodynamics effects produced by plunging foil in a fluid," *Chemical and Processing Engineering*, vol. 31, pp. 579-588, 2010
[19] Martin, C., Tun, R., Castelli, V., "The DARPA Nano Air Vehicle Program," *AIAA online proceedings*, AIAA 2012-0583, http://dx.doi.org/10.2514/6.2012-583, 2012.
[20] Mwongera, V., M., "A review of Flapping Wing MAV modelling," *International Journal of Aeronautical Sciences and Aerospace Research,"* , Vol. 2, No. 2, April 2015, pp. 17 – 26.
[21] Ol, M. V., Unsteady low Reynolds number aerodynamics for micro air vehicles (MAVs), AFRL-RB-WP-TR-2010-3013, 2010.
[22] Ol. M. V., (Editor), Unsteady Aerodynamics for Micro Air Vehicles, RTO AC/323(AVT-149)TP/332 ISBN 978-92-837-0118-7, 2010.
[23] Ramamurti, R., Sandberg, W. C., "A Computational Study of the Aerodynamics of Hovering and Maneuvering in Drosophila," *AIAA online proceedings*, http://dx.doi.org/10.2514/6.2007-669.
[24] Ramamurti, R., Sandberg, W. C., "A three-dimensional computational study of the aerodynamic mechanisms of insect flight," *The Journal of Experimental Biology* , no. 205, 2002, pp. 1507-1518.
[25] van den Berg, C., Ellington, C. P., "The three-dimensional leading-edge vortex of a hovering model hawkmoth," *Phil. Trans. R. Soc. London*, B, 1997.
[26] Wang, J., Birch, M., Dickinson, H., "Unsteady forces and flows in low Reynolds number hovering flight: two-dimensional computations *vs* robotic wing experiments," *The Journal of Experimental Biology*, 207, ppp. 449-460, 2000.

Copyright Statement